

# Extreme wave events and sampling variability

Elzbieta M. Bitner-Gregersen<sup>1</sup>, Odin Gramstad<sup>1</sup>,  
Anne Karin Magnusson<sup>2</sup>, Mika Malila<sup>2</sup>



12 November 2019

**2nd International Workshop on Waves, Storm Surges and Coastal Hazards**  
***Incorporating the 16 International Waves Workshop***

10–15 November 2019, Melbourne, Australia

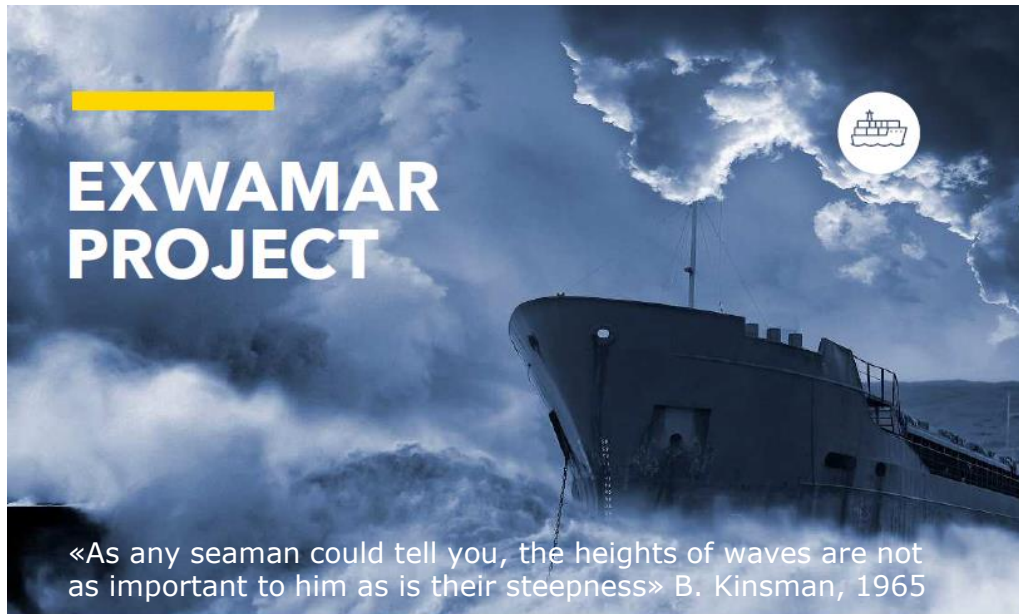




- **Research project (2016-2019)**

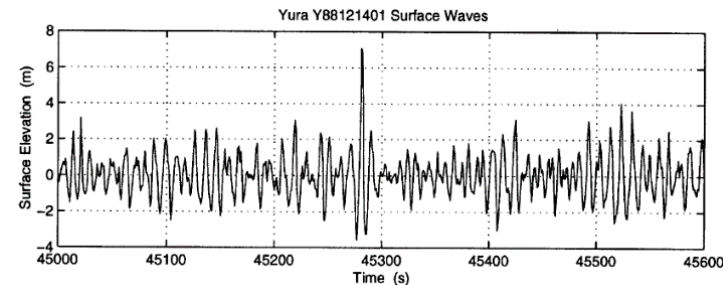
- **Partners:** [DNV GL](#), Norwegian Meteorological Institute, University of Oslo (Department of Mathematics)

- **Funded partly by RCN**  Forskningsrådet



- **Overall objectives:**

- To develop improved **warning criteria** indicating increased risk of extreme or rogue waves for the shipping and offshore industries.
- To develop **DNV GL HOSM** (Higher Order Spectral Method) code based on the methodology due to Dommermuth and Yue (1989) and West et al. (1989).



Yura wave recorded in Sea of Japan (Mori et al. 2003)

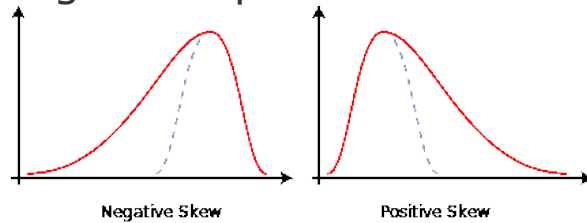
- **ConocoPhillips** is acknowledged for providing Ekofisk field data used in ExWaMar

# Background

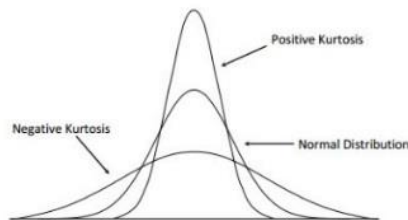
## for given strong focus to sampling variability in ExWaMar

❖ **Linear irregular waves are Gaussian distributed**, a measure of **nonlinearity** - deviation from the Gaussian distribution of a **surface elevation pdf**

▪ **Skewness**, a measure of the asymmetry of the sea surface elevation pdf, primarily the **second order effect**. A positive skewness - higher wave crests and shallower wave troughs compared to the linear wave model.



▪ **Kurtosis**, primarily the **third order effect** and a descriptor of the shape of the surface elevation pdf. A kurtosis coefficient larger than three indicates more extreme waves.



❖ **Mechanisms for the formation of rogue waves** (see e.g. Onorato, 2013, Bitner-Gregersen and Gramstad, 2016; Osborne, 2010):

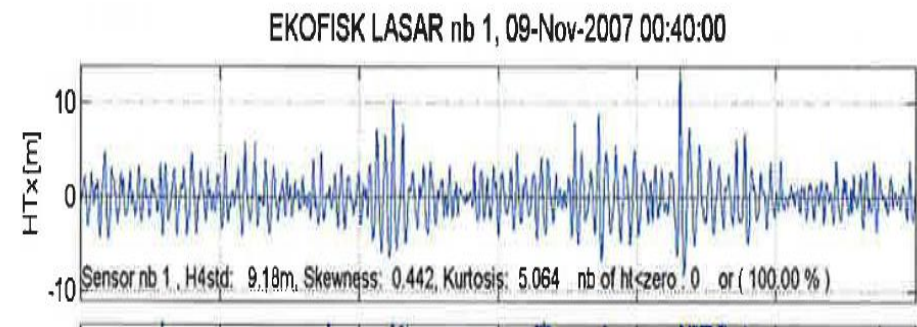
- linear Fourier superposition (frequency or angular linear focussing); wave-current interaction; nonlinear quasi-resonance interactions (modulational instability); crossing seas; shallow water effects; wind

❖ **Donelan & Magnusson (2017) – Andrea wave, Nov., 9, 2007 at 00:40 UTC**

❖  $H_{m0}=9.18\text{m}$ ;  $T_p=13.2\text{s}$ ;  $k_p H_s/2=0.11$

$C_{max}/H_s=1.63$

**Kurtosis > 4.0**



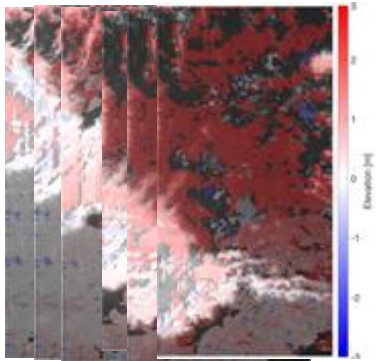
# Area effects on wave characteristics

- Focus given to rogue-prone sea states and numerical simulations. Field data from the Ekofisk field.

## Ekofisk 2/4 Kilo - a wave laboratory



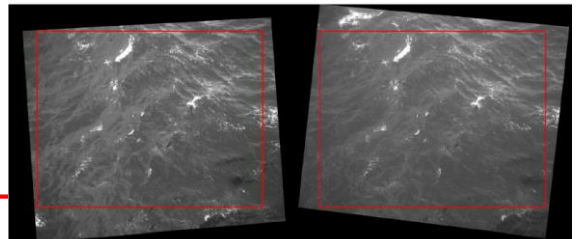
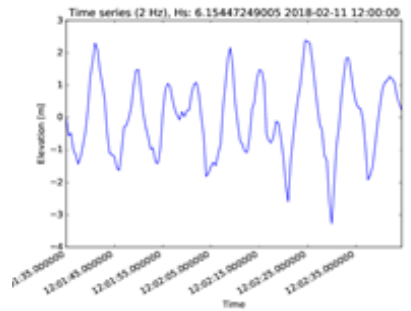
Stereo video



WaMoS



LASAR





# Sampling variability

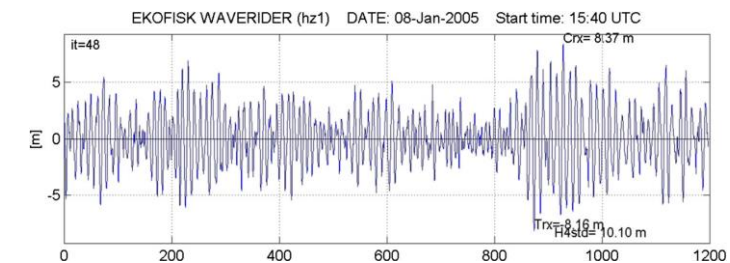
## Uncertainties

- **Aleatory uncertainty** represents a natural randomness of waves, also known as intrinsic or inherent uncertainty, cannot be reduced or eliminated.
- **Epistemic uncertainty** represents errors which can be reduced by collecting more information about a considered quantity.
- Data uncertainty
- Model uncertainty
- Statistical uncertainty (**sampling variability**) due to limited number of observations:

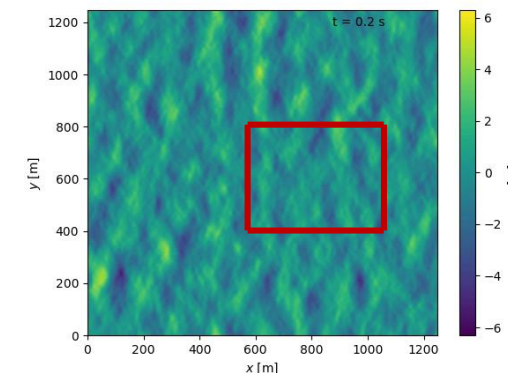
Longuet-Higgins (1952), Lipa et al. (1981), Donelan & Pierson (1983), Young (1986), *Monaldo* (1988), Bitner-Gregersen & Hagen (1990), Tucker (1992), and Forristall et al. (1996), among others.

Piterbarg (1996), Krogstad et al. (2004), Socquet-Juglard et al. (2005), Forristall (2011, 2015), Benetazzo et al. (2006, 2015), Hagen et al. (2018)

- **Temporal observations** – duration of a wave record (see e.g. Bitner-Gregersen (2003), Bitner-Gregersen & Hagen, 2003; Bitner-Gregersen & Magnusson, 2014).



- **Spatial observations** – dimension of an ocean area and duration of observations



If the sampling rate is the same, more space-time data than single-point data

# Set up of numerical simulations

- Numerical simulations carried out using a numerical solver based on the **Higher Order Spectral Method (HOSM)**, first proposed by Dommermuth and Yue (1989) and West et al. (1989).
- The nonlinear order  $M$  in the **HOSM simulations** was in this study set to  **$M=3$** , which includes the leading order nonlinear dynamical effects, including the effect of modulational instability.
- **Unidirectional** and **directional wave fields in deep water** have been simulated in a spatial domain with periodic boundary conditions.
- For the **unidirectional simulations**, the spatial domain was discretized by  **$n_x = 1024$  grid points**, while in the **short-crested simulations** the horizontal plane was discretized using  **$n_x=n_y$  512 x 512 grid points**.

- In the simulations, the initial condition was chosen as a wave system with the Pierson-Moskowitz (**PM**) or the **JONSWAP spectrum** and with directional spreading function  $\cos^N(\phi - \phi_p)$ .

- The wave spectrum was defined as  $E(k) = F(k)D(\phi)$

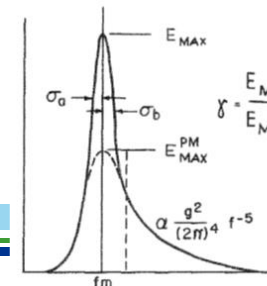
$$F(k) = \frac{\alpha}{2k^3} \exp\left[-\frac{5}{4}\left(k/k_p\right)^{-2}\right] \gamma \exp\left[-\frac{(\sqrt{k/k_p}-1)^2}{2\sigma^2}\right]$$

$$D(\phi) = \frac{1}{k\sqrt{\pi}} \frac{\Gamma(N/2+1)}{\Gamma(N/2+1/2)} \cos^N(\phi - \phi_p), \quad \text{if } |\phi - \phi_p| \leq \frac{\pi}{2}$$

$$D(\phi) = 0$$

otherwise

- $\gamma=1, 2, 3.3$  and **6**, used in the analysis.  $\gamma=1$  the JONSWAP spectrum reduces to the PM spectrum.

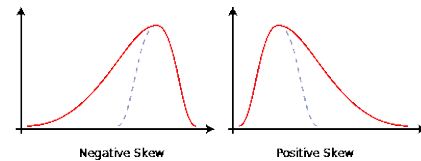


# Parameters and sea states investigated

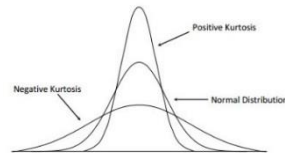
- For a surface snapshot from the numerical simulations  $\eta_{i,j} = \eta(x_i, x_j)$  where  $i=1, \dots, n_x$  and  $j=1, \dots, n_y$  (here  $n_x = n_y = 512$ ).

- The sample **skewness**  $\kappa_3$  and **kurtosis**  $\kappa_4$  defined

$$\kappa_3 = \frac{\frac{1}{n_x n_y} \sum_{i=1}^{n_x} \sum_{j=1}^{n_y} (\eta_{i,j} - \overline{\eta_{i,j}})^3}{\left( \frac{1}{n_x n_y} \sum_{i=1}^{n_x} \sum_{j=1}^{n_y} (\eta_{i,j} - \overline{\eta_{i,j}})^2 \right)^{3/2}}$$



$$\kappa_4 = \frac{\frac{1}{n_x n_y} \sum_{i=1}^{n_x} \sum_{j=1}^{n_y} (\eta_{i,j} - \overline{\eta_{i,j}})^4}{\left( \frac{1}{n_x n_y} \sum_{i=1}^{n_x} \sum_{j=1}^{n_y} (\eta_{i,j} - \overline{\eta_{i,j}})^2 \right)^2}$$



- The **maximum surface elevation**  $\eta_{max} (C_{max})$
- The coefficient  $\kappa_3$  and  $\kappa_4$  and  $\eta_{max}$  are calculated as averages over all random realizations of the same sea state. **1800s** unidirectional HOSM simulations were repeated **1000 times**, directional **20 times**.

- The Andrea and Justine Three Sisters sea states

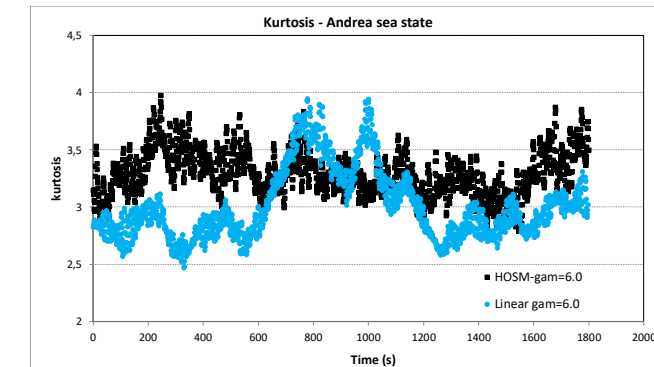
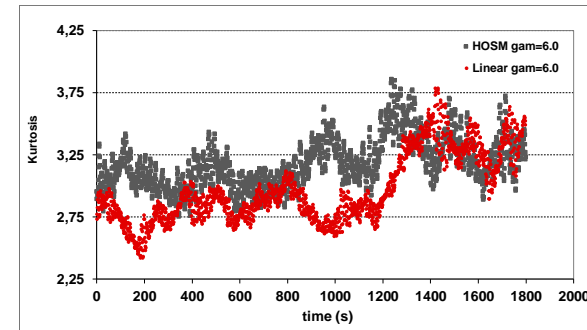
Case	Date and time	$H_{m0}$ (m)	$T_p$ (s)	Wave Steepness
1	1 Jan. 1995, 15:20 UTC	11.2	16.7	0.08
2	5 Feb. 1999, 04:40 UTC	7.6	13.0	0.09
3	27 Dec. 1998, 06:40 UTC	10.4	14.6	0.10
4	25 Oct. 1998, 16:00 UTC	8.8	12.6	0.11
5	1 Dec. 1999, 02:20 UTC	7.2	11.3	0.11
6	1 Jan. 1995, 23:00 UTC	5.7	9.8	0.12
7	Numerical simulations	6.5	10.0	0.13
8	Numerical simulations	6.9	10.0	0.14
9	29 Jan. 2000, 18:40 UTC	12.1	12.2	0.16

# Sampling variability

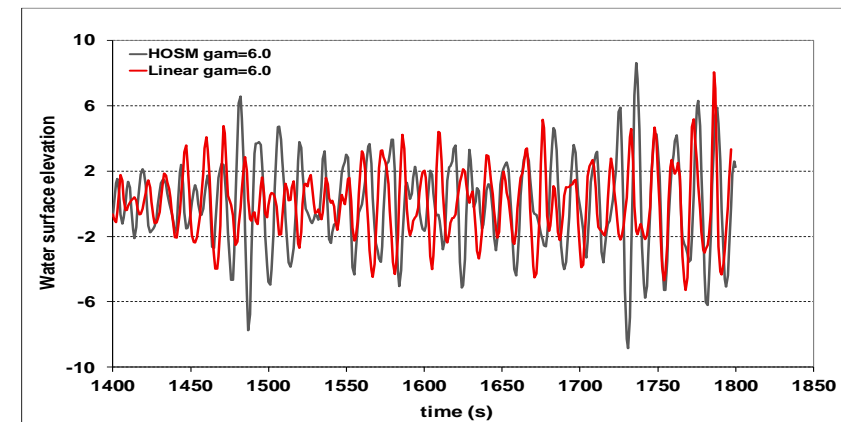
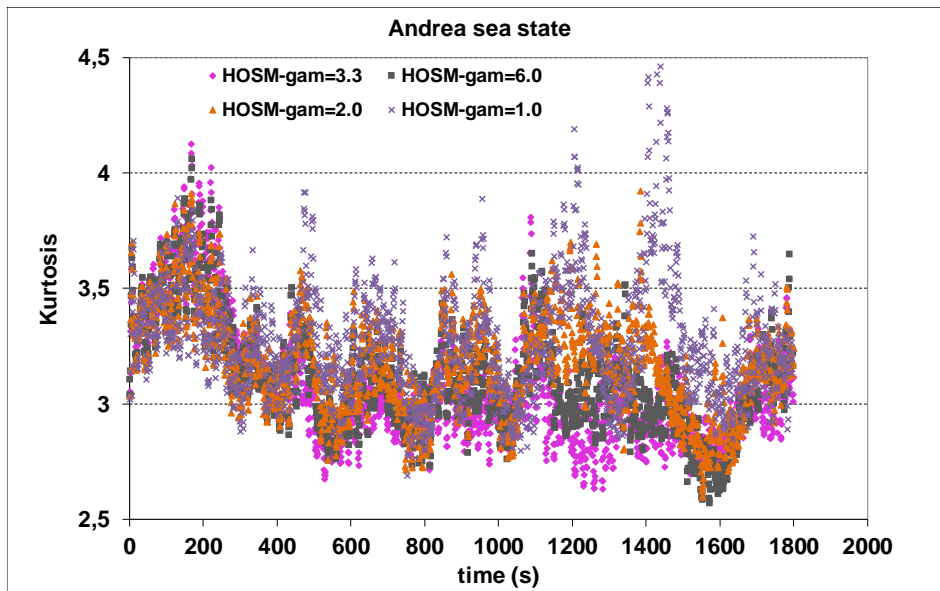
Andrea sea state  $H_s=9.2$  m and  $T_p=13.2$  s,  $k_p H_s/2=0.11$ ; unidirectional waves

- Modulational instability in **deep** and **intermediate water** characterized by high wave steepness and a narrow wave spectrum (in frequency and direction) and can be parameterized by **the Benjamin-Feir Index (BFI)**, see e.g. Onorato et al. (2006)
- Expected that the **JONSWAP spectrum** with  $\gamma=6$  will generate higher  $K_3$  and  $K_4$  than PM one with  $\gamma=1$ , given the two spectra have the same  $k_p H_s/2$

- Unidir. linear and HOSM waves, **JONSWAP  $\gamma=6$** , given seed



- Evolution of the wave train**

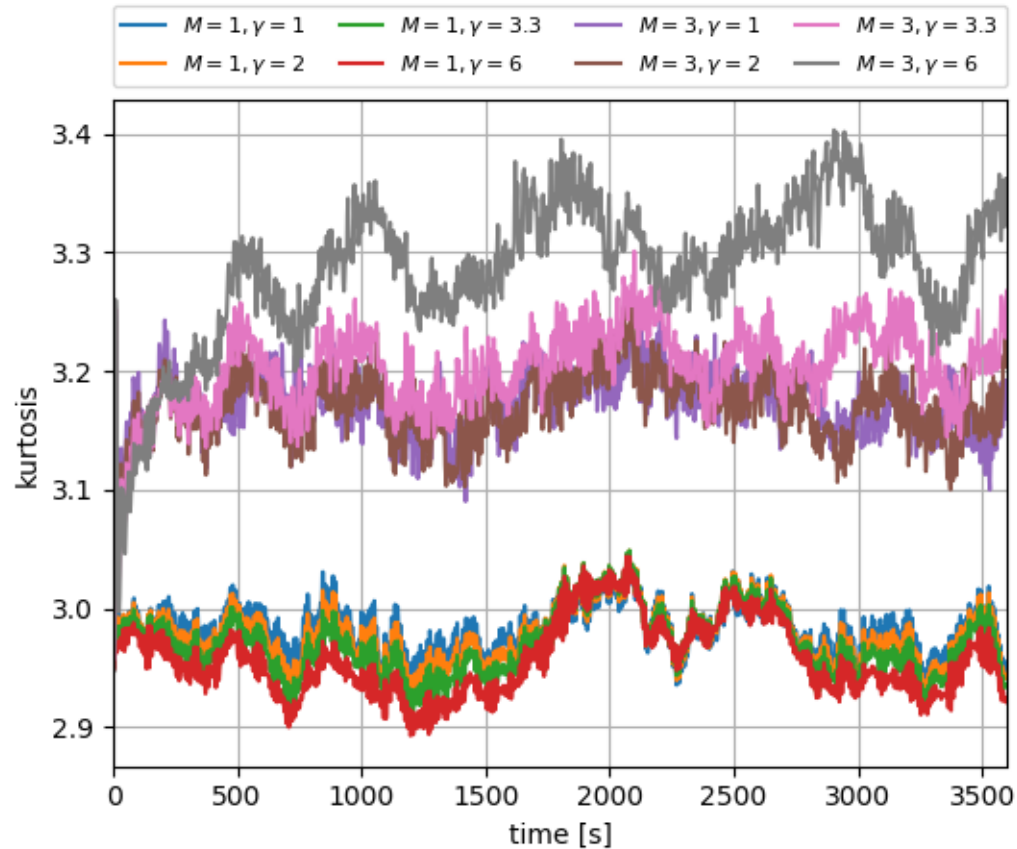




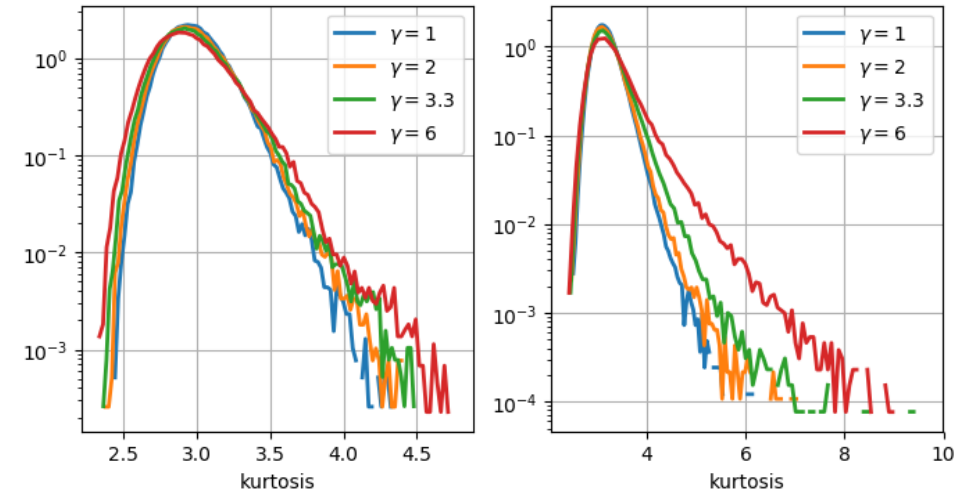
# Sampling variability

## Andrea sea state, unidirectional waves; $k_p H_s / 2 = 0.11$

Estimated HOSM spatial kurtosis as a function of simulation time.



- Distribution of kurtosis** derived from unidirectional linear (left) and nonlinear,  $M=3$ , (right) simulations,  $H_s = 4.0$  m and  $T_p = 10$  s,  $k_p H_s / 2 = 0.11$ , **100 runs**.



M	$\Gamma$	Mean	Std
1	1.0	2.98	0.19
1	2.0	2.98	0.21
1	3.3	2.97	0.22
1	6.0	2.96	0.24
3	1.0	3.17	0.26
3	2.0	3.17	0.28
3	3.3	3.20	0.34
3	6.0	3.29	0.47

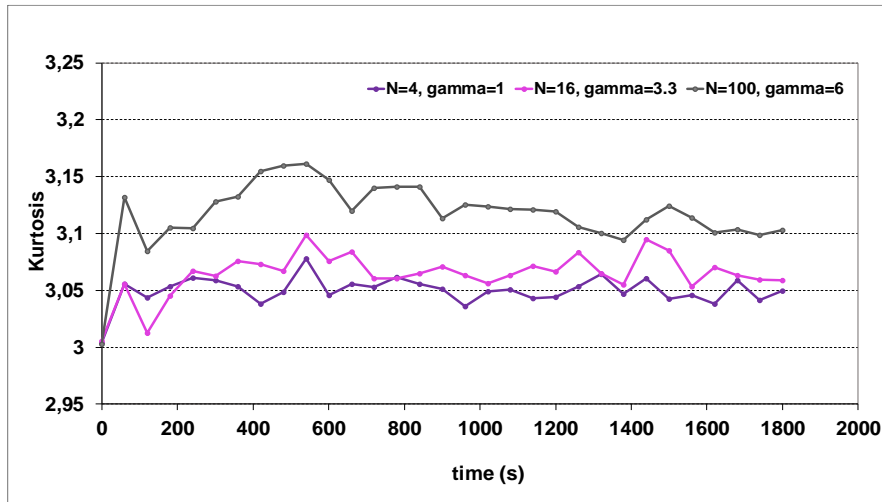
# Sampling variability

## Directional waves, $H_s=5.66$ m and $T_p= 10$ s, $k_p H_s/2=0.10$

- Sea states considered in the analysis,  $k_p H_s/2=0.10$ ;  $N=4, 16, 100$ .

Case	$\gamma$	N	$H_s$	$T_p$
1	1.0	4	5.66 m	10 s
2	3.3	16	5.66 m	10 s
3	6.0	100	5.66 m	10s

- Estimated ***K4*** as a function of time, 20 repetitions of the 30-minute HOSM simulations.



- Mean and standard deviation of kurtosis, directional wave field

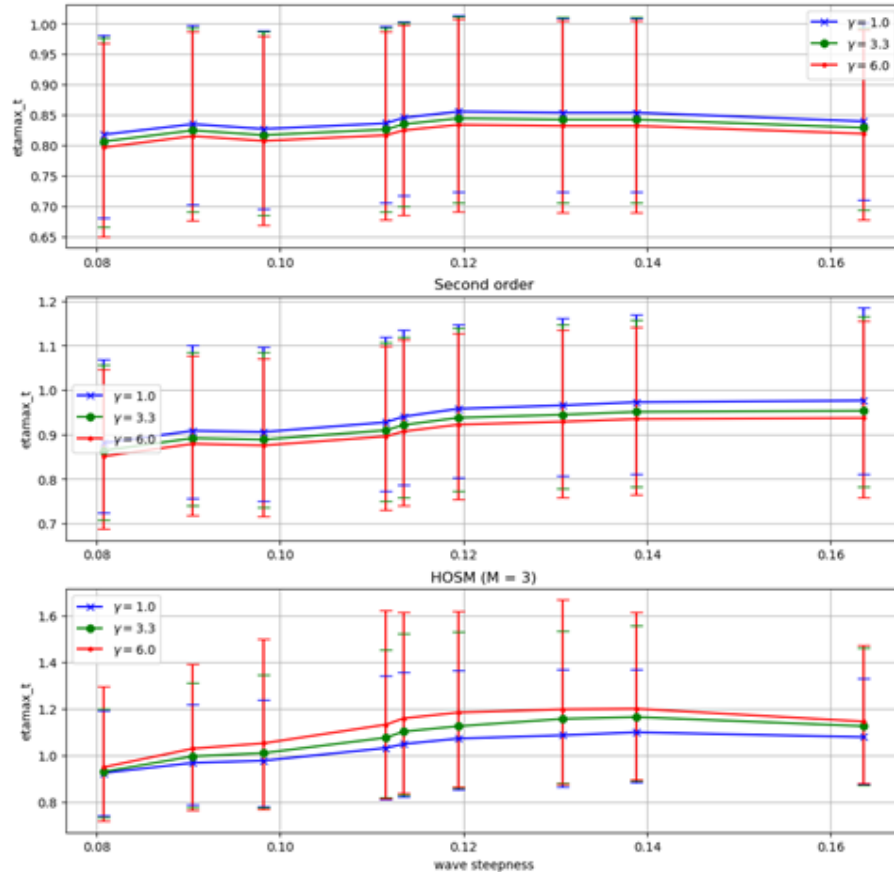
M	$\Gamma$	N	Mean	Std
3	1.0	4	3.05	0.04
3	3.3	16	3.07	0.06
3	6.0	100	3.12	0.11

- The **sampling variability of kurtosis**, expressed in terms of the **standard deviation (Std)**, is the **highest for the JONSWAP spectrum with  $\gamma=6$  and  $N=100$**  (nearly unidirectional waves), followed by  $\gamma=3.3, N=16$  and  $\gamma=1, N=4$ .

# Numerical results - $\eta_{max}/H_s$

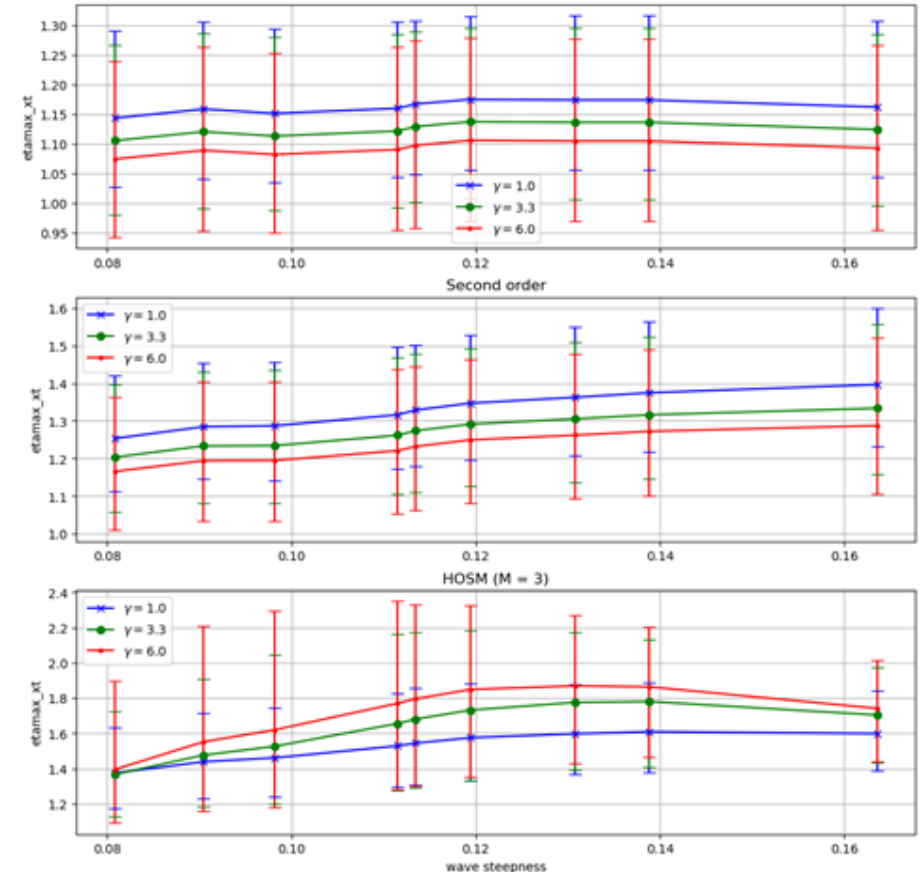
- Simulated unidirectional wave records are shown for the sea states with the wave steepness  $kpH_s/2=0.08, 0.09, \dots, 0.14, 0.16$ .

## Temporal



- The results of linear, 2<sup>nd</sup> order and HOSM simulations with Jonswap spectrum with gamma parameter  $\gamma=1.0, 3.3$  and  $6.0$ .

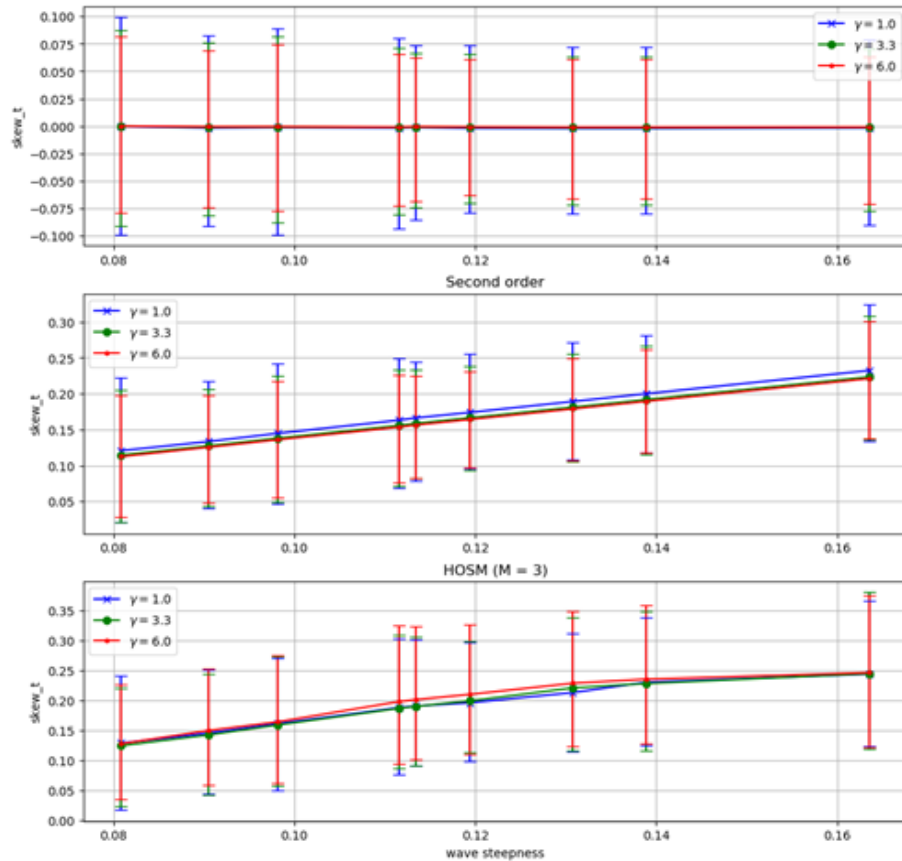
## Spatial



# Numerical results – skewness $\kappa_3$

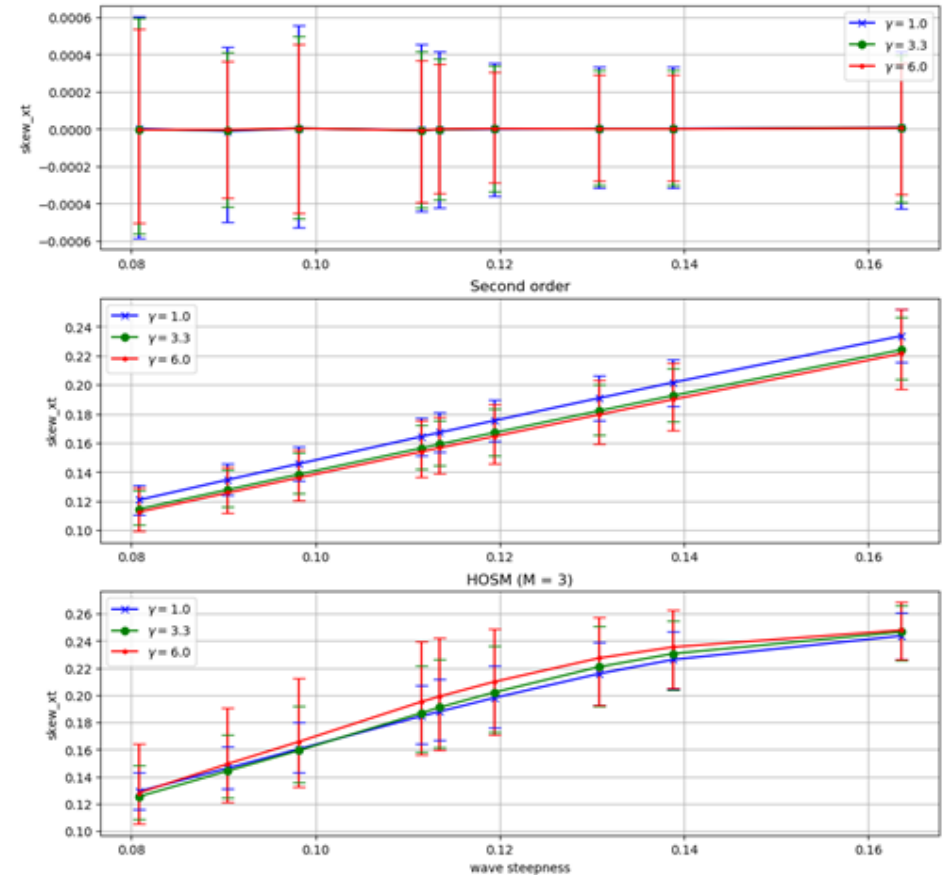
- Simulated unidirectional wave records are shown for the sea states with the wave steepness  $kpHs/2=0.08, 0.09, \dots, 0.14, 0.16$ .

## Temporal



- The results of linear, 2<sup>nd</sup> order and HOSM simulations with Jonswap spectrum with gamma parameter  $\gamma=1.0, 3.3$  and 6.0.

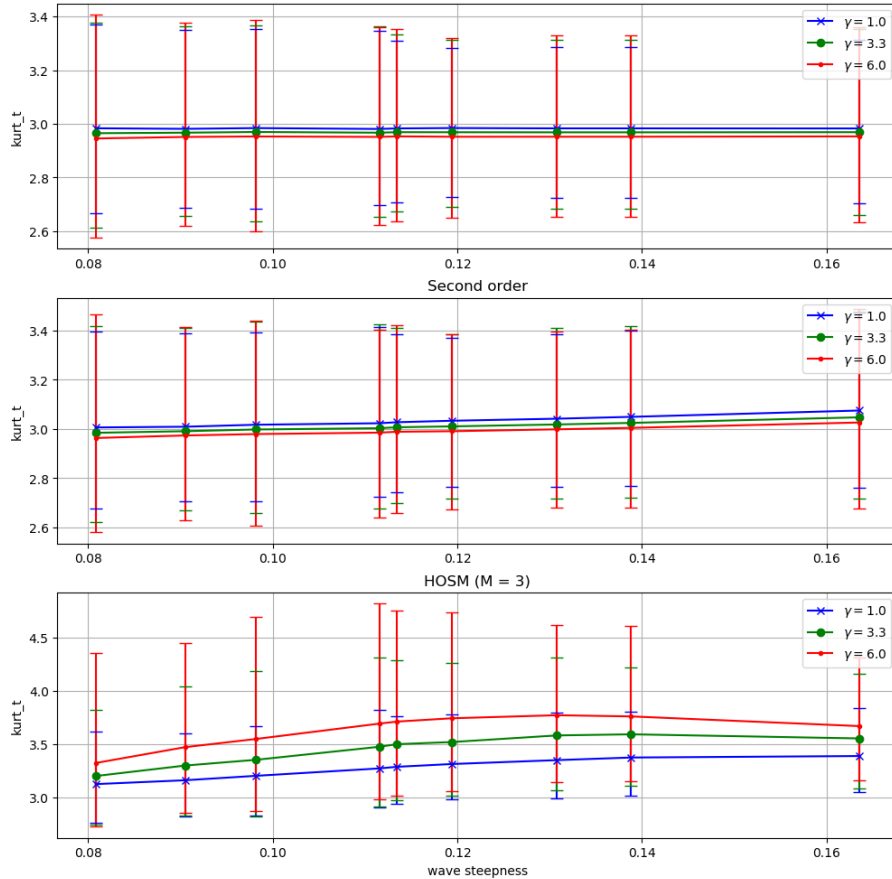
## Spatial



# Numerical results – kurtosis $\kappa_4$

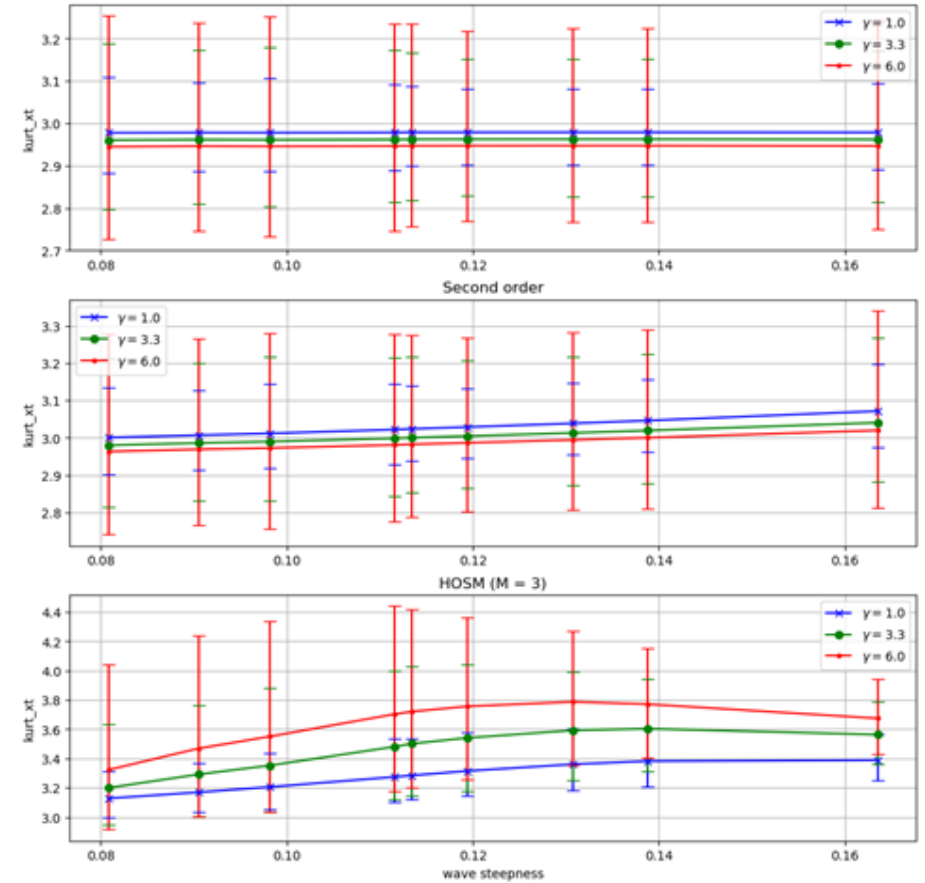
- Simulated unidirectional wave records are shown for the sea states with the wave steepness  $kpHs/2=0.08, 0.09, \dots, 0.14, 0.16$ .

## Temporal



- The results of linear, 2<sup>nd</sup> order and HOSM simulations with Jonswap spectrum with gamma  $\gamma=1.0, 3.3$  and 6.0.

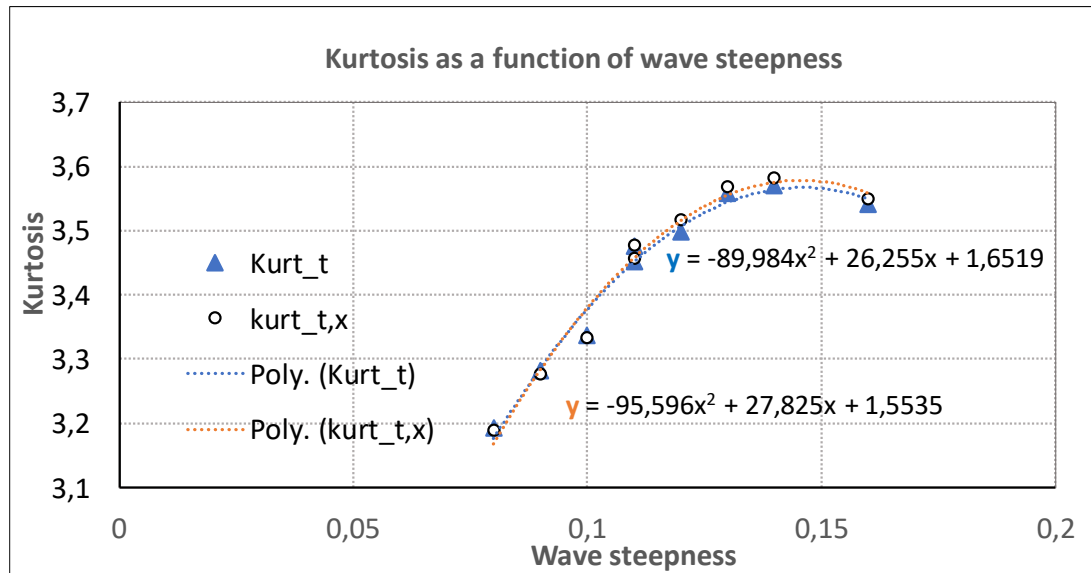
## Spatial





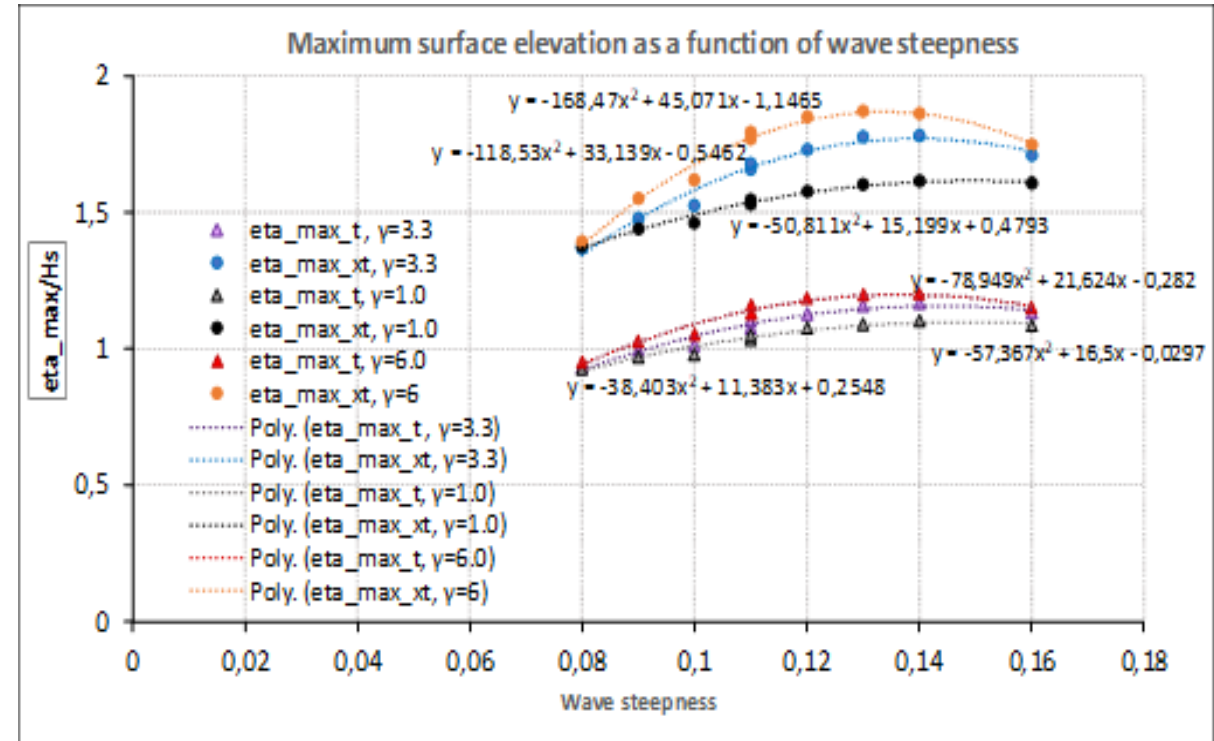
# Average temporal and spatial estimators

- Average (over all random realizations of the same sea states) temporal/spatial **kurtosis** as a function of wave steepness



- Temporal/spatial **kurtosis** is also approx. equal. COV up to 0.16 for temporal, and 0.12 for spatial data.

- $\eta_{max}/H_s$  as a function of wave steepness



- The spatial  $\eta_{max}/H_s$  differs significantly from the temporal one as the spatial calculation covers many more waves than the single point measurement.

# Average time-space kurtosis

- Kurtosis  $\kappa_4$  (Mori & Jansen, 2006; Mori et al., 2011; Janssen & Janssen, 2019)

$$\kappa_4 = 3 + \kappa_4^{(bound)} + \kappa_4^{(dyn)}$$

For narrow band waves in deep water according to Janssen (2009)

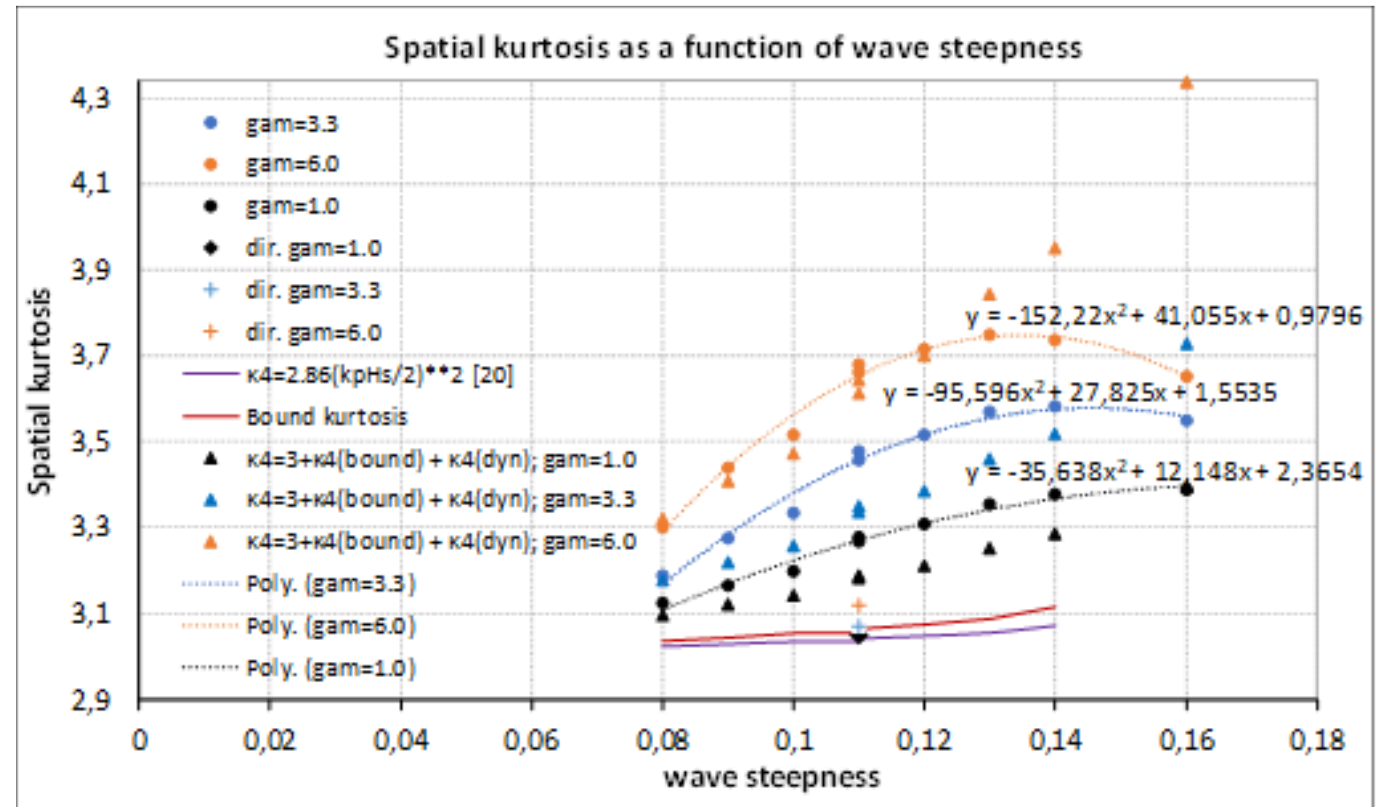
$$\kappa_4^{(bound)} = 4.5(k_p H_s / 2)^2$$

For unidirectional narrow band waves and Gaussian spectrum, from numerical simulations of the MNL Schrödinger Equations Mori et al. (2011) showed

$$\kappa_4^{(dyn)} = (\pi / \sqrt{3}) BFI^2$$

where BFI is the Benjamin-Feir Index (see Onorato et al., 2006)

- Average spatial skewness as a function of wave steepness, HOSM simulations



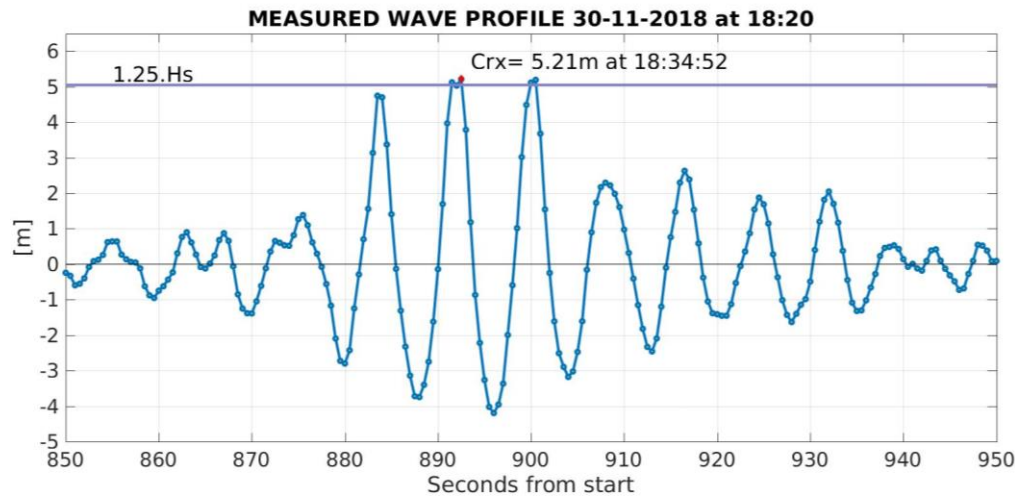
# Justine Three Sisters and HOSM simulations

- Justine Three Sisters, Magnusson et al. (2019)

Sea state  $H_s=4.0\text{m}$ ,  $T_p=8.39\text{s}$

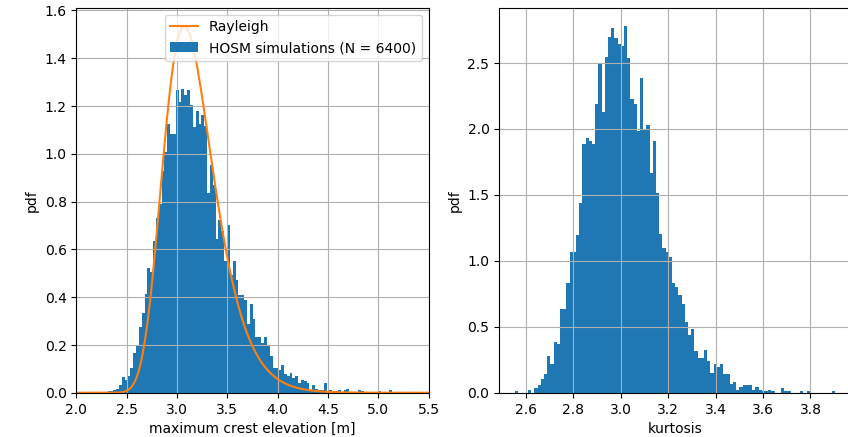
$C_{max}/H_s=1.30$  to  $1.41$

$H_{max}/H_s=2.35$  to  $2.54$

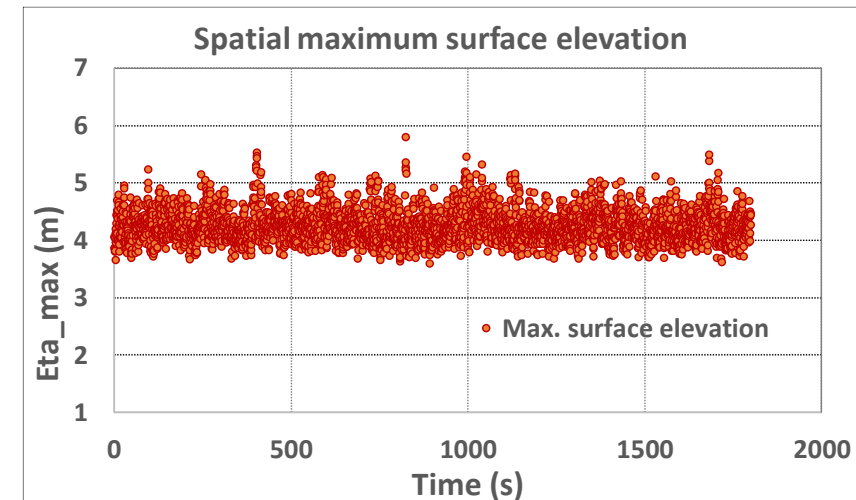


- HOSM in an area of  $3.5\text{ km} \times 3.5\text{ km}$ , and 256 30-min. wave records (time series) were extracted from each simulation, 30 runs ( $30 \times 256$ ). The crest height of  $5.2\text{ m}$  reproduced in several runs with different seeds

- Time simulations

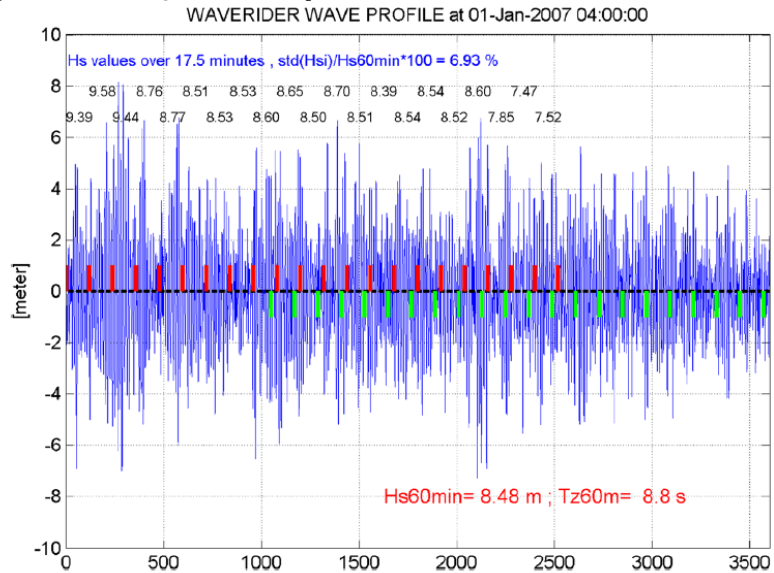


- Spatial maximum crest



# Single point field data Jan. 2016 – Sept.2019

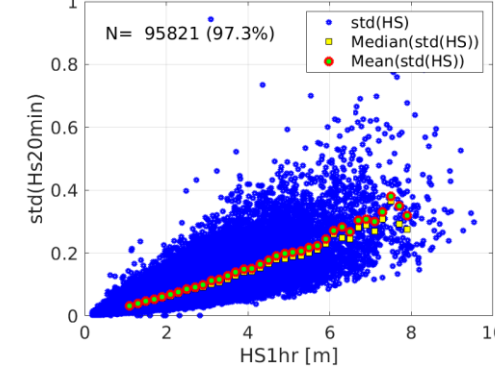
- The adopted approach (Bitner-Gregersen & Magnusson, 2014).



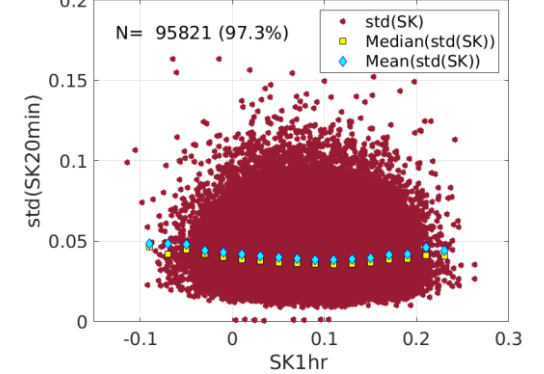
- Red bars are start points of each 20-min records, and green bars (downwards) show the end of them. Centered in the hour, there are 20 records with 20min of data at all steps of 1min to the left and to the right. Including the center one, that makes 41 20-minutes records to evaluate a standard deviation of the parameters

- Hs, skewness, kurtosis**

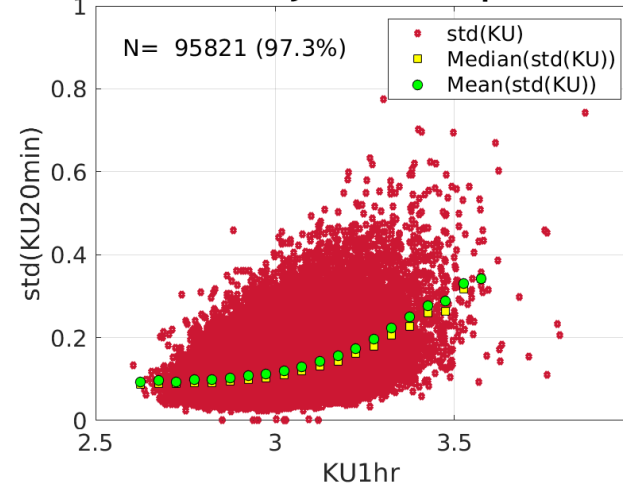
SIGNIFICANT WAVE HEIGHT Jan 2016 - Sept 201



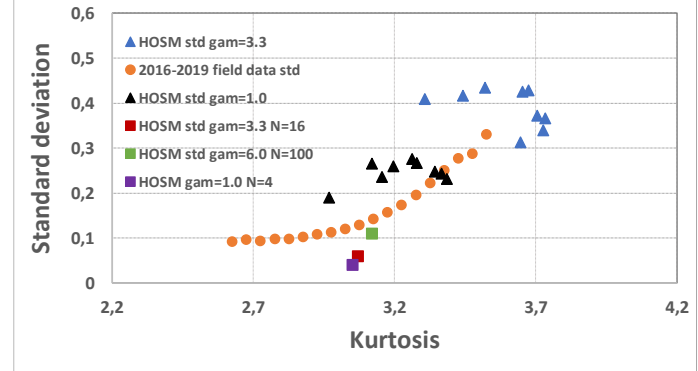
SKEWNESS Jan 2016 - Sept 2019



KURTOSIS Jan 2016 - Sept 2019

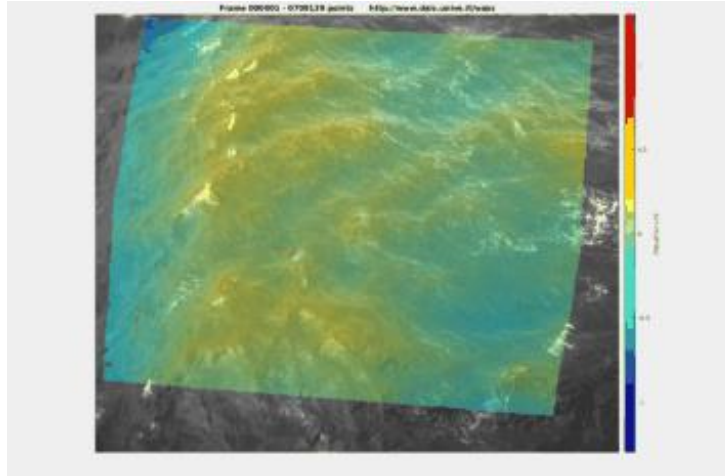


Standard deviation of kurtosis



# Ekofisk Stereo Video system on EKO-K

- A 1-minute sequence of stereo images from Ekofisk, processed with the WASS software, (Bergamasco et al., 2017)



- The setup which only covered a small (roughly 20\*20 m) area. Our new setup covers a much larger area (large enough to fully resolve most if not all possible wavelengths)

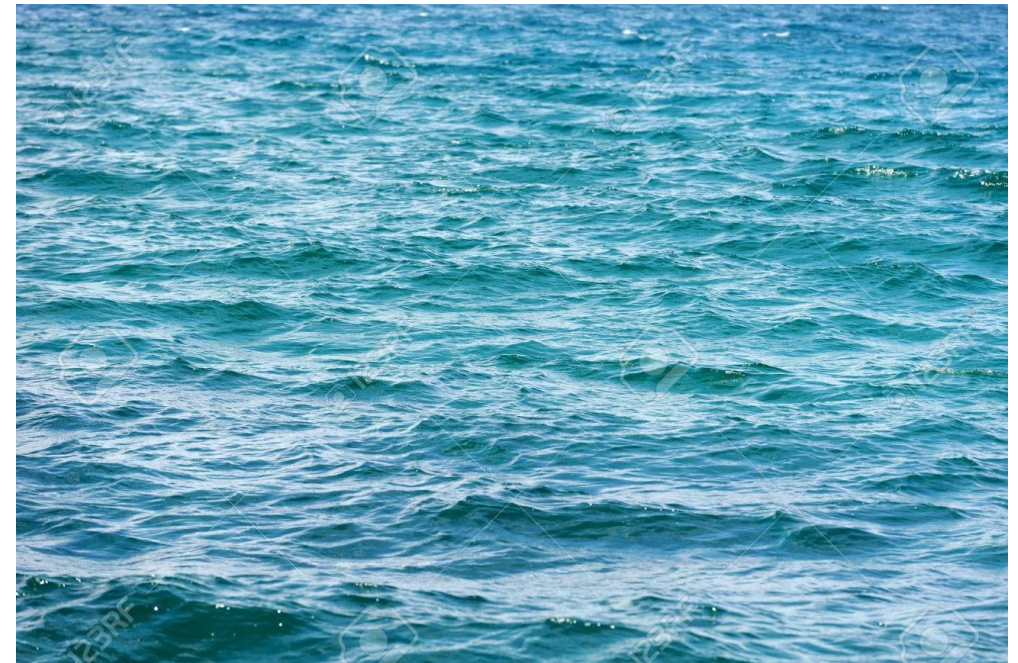
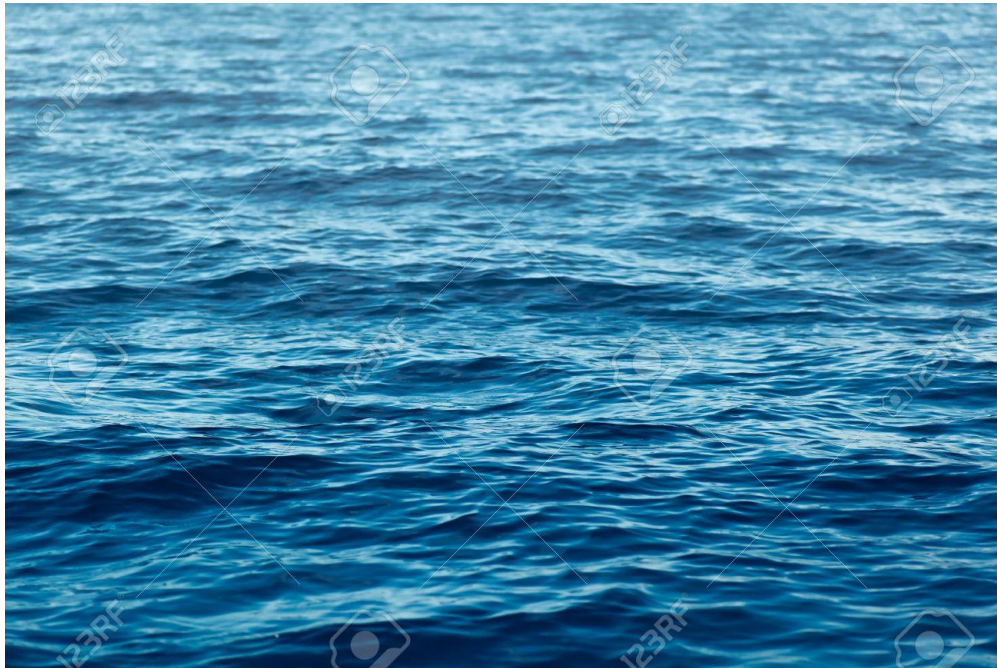


# Conclusions

- Numerical simulations show that a **nonlinear wave field including dynamical effects is more sensitive to sampling variability** than the 2<sup>nd</sup> order and linear one. The shape of a wave spectrum does not affect much skewness but impacts kurtosis and  $\eta_{max}$ . Directionality reduces significantly nonlinearities.
- Based on statistical sea state wave characteristics it is **not possible to conclude on degree of nonlinearity of a wave train**, due to sampling variability. Numerical models and laboratory experiments represent supporting tools to field data. Duration of wave records and dimensions of an ocean area is essential for wave statistics.
- **For the same sampling rate there will be more space-time data than single-point** data which will be less affected by sampling variability. Therefore, **probability of occurrence of rogue waves is higher in field space data than in time observations.**
- If **duration of observations is long** and we consider **a large ocean area estimates** of wave characteristics in time will be equal to space-time ones.
- **Field data support findings** showing significant impact of sampling variability on wave characteristics of a sea state.
- **The Norwegian Standard NORSOK (2017)** recommends a **10% increase** in estimated extreme crest height compared to 2<sup>nd</sup> order point statistics.
- **Theoretical expressions for kurtosis** derived by Jansen (2009) Mori et al. (2011), Jansen & Jansen (2019) for Gaussian spectrum do **not provide satisfactory results** when applied to the JONSWAP and P-M spectrum.

# Sampling variability

**THANK YOU FOR YOUR ATTENTION**



# Sampling variability

**Trondheim Workshop, 21-22 Oct. 2019**

DNV GL

Høvik, Norway

**[www.dnvgl.com](http://www.dnvgl.com)**

**SAFER, SMARTER, GREENER**

The trademarks DNV GL®, DNV®, the Horizon Graphic and Det Norske Veritas® are the properties of companies in the Det Norske Veritas group. All rights reserved.